A general multiaxial method to estimate the local elastic-plastic behavior from a purely elastic solution

R. J. McDonald and D. F. Socie

Department of Mechanical Science and Engineering, University of Illinois at Urbana-Champaign, 1206 West Green Street, Urbana, Illinois 61801, USA

Email: rjmcdona@illinois.edu, dsocie@illinois.edu

ABSTRACT. *In most fatigue applications, the nominal structural behavior is dominated by elastic deformation, but the fatigue lifetime is significantly influenced by plasticity around stress concentrations and flaws. Although the elastic-plastic behavior can be modeled with finite element analysis (FEA), the computational expense may be prohibitive, especially for variable amplitude loading with multiaxial stress states. To overcome this complexity, a local elastic-plastic estimate is explored that utilizes the purely elastic solution. The method is conceptually similar to previous work, but is adapted to be consistent for variable amplitude multiaxial cyclic loading histories. This approach combines a magnitude criterion (i.e. Neuber [1] or ESED [2]), the Masing character of the pseudo-material method [9-10], and has the generality to adopt any appropriate multiaxial plasticity model. The assumptions of the current approximation are developed in a general manner, with the potential to adjust the constraint (i.e. direction alignment), magnitude, and the plasticity character as necessary.*

INTRODUCTION

Many fatigue applications would benefit from improved estimates in the mechanical response, particularly for short-moderate lifetimes where plastic deformation dominates the material damage. In recent years, the finite element method has been utilized successfully in a wide variety of circumstances, including cyclic fatigue application. However, cyclic deformation using FEM remains costly, particularly for non-proportional multiaxial cyclic loading histories. In an attempt to address this prohibitive cost, an elastic-plastic approximation based on the local elastic (i.e. FEM) is one practical solution to obtain sufficient predictive capabilities.

Much of the previous work to obtain an elastic-plastic estimate is based on stress concentration factors around notches. The most common of these estimates was developed by Neuber [1] in 1961, when he related the stress and strain concentration factors to the elastic behavior. Another popular approach was introduced by Molski and Glinka [2], which equates the strain energy density between the purely elastic and elastic-plastic approximation (ESED). Both of these methods have been the involved in several other investigations [3-8], but their extension to non-proportional multiaxial loading is fairly limited. For instance, applying the ESED method to multiaxial loading [4] can result in a multiple solutions. Consequentially, a procedure to determine the correct (or most appropriate) solution must be adopted. This ambiguity and the restriction of potential plasticity models limit the applications of typical ESED methods.

A pseudo-material approach [9-10] has been more successful in achieving appropriate estimates for general non-proportional multiaxial loadings. This method involves assuming that the notched material behaves similar to the real material (with modification of material parameters, or potentially the material model). The advantage of the pseudo-material method is its familiar construction and straightforward application to non-proportional multiaxial loading. The difficulty of these methods is choosing an appropriate pseudo-material model because either the notch geometry (or elastic solution's mechanical behavior) is coupled to the true material response to estimate the local strains. Although such an avenue would be ideal with limited notches geometries and sufficient experiments, its non-trivial coupling makes modifying assumptions for different applications non-trivial. For example, this coupling requires special consideration to translate the hydrostatic response, because of the elastic solution tends to over-estimate volume changes. Furthermore, the pseudo-material approach is not necessarily compatible with the familiar relationships (such as Neuber or ESED) and the solution requires solving the plasticity problem twice.

In the current investigation, a method is proposed to estimate the elastic-plastic behavior from a purely elastic solution by adopting a directional alignment and applying a magnitude condition as a modified boundary condition. The result is a method that maintains the multiaxial advantages of the pseudo-material approach, but uncouples the geometrical and local material behavior to simplify the assumptions involved in approximating the elastic-plastic deformation.

MATERIAL MODELING

In the classic notch-problem, determining the stress concentration factor (i.e., from elastic solutions, experimental techniques, or the FEM) is often the first step to estimate the local elastic-plastic behavior. Due to the overwhelming popularity of the finite element method, it is advantageous to utilize the local purely elastic solution (rather than the nominal loading) to further generalize the elastic-plastic estimate. Although utilizing the local elastic solution greatly simplifies the notch problem, several assumptions are still required to acquire meaningful elastic-plastic approximations. For instance, consider a general local solid mechanics problem with 12 unknowns (6 stresses and 6 strains) at a single material point. The elastic-plastic estimate is obtained by approximating these unknowns through an appropriate material model (6 relationships) and the purely elastic solution (6 components). In this investigation, the material's constitutive behavior and geometry are considered independently to construct an approximation technique that is appropriate to multi-axial fatigue loading.

Since cyclic deformation is of primary interest, the total strain increment, $\Delta\boldsymbol{\varepsilon}$, is additively constructed from the elastic, $\Delta\boldsymbol{\varepsilon}^e$, and plastic, $\Delta\boldsymbol{\varepsilon}^p$, strain increments, which is appropriate for small strain deformation (i.e. $\|\boldsymbol{\varepsilon}\|<<1$)

$$\Delta\boldsymbol{\varepsilon} = \Delta\boldsymbol{\varepsilon}^e + \Delta\boldsymbol{\varepsilon}^p \quad (1)$$

An incremental format was adopted because only rate independent deformation is considered in the current investigation. The elastic strain increment is related to the stress increment by isotropic linear elasticity (Hooke's Law [11]):

$$\Delta\boldsymbol{\varepsilon}^{e} = \frac{1}{2\mu}\Delta\boldsymbol{\sigma}' + \frac{1}{9\kappa}\mathrm{tr}\left(\Delta\boldsymbol{\sigma}\right)\mathbf{I} \tag{2}$$

where $\mathbf{I}$ is the 2nd order identity tensor and the trace, tr($\mathbf{x}$), is defined as:

$$\mathrm{tr}\left(\mathbf{x}\right) = x_{11} + x_{22} + x_{33}. \tag{3}$$

This elasticity format was chosen because it decouples the deviatoric, $\Delta\boldsymbol{\sigma}'$, and hydrostatic, tr($\Delta\boldsymbol{\sigma}$), stress contributions with the shear, μ, and bulk, κ, moduli, respectively, which is advantageous when considering volume conserving plastic deformation. The plastic strain increment is characterized by a plastic strain magnitude, $d\lambda$, and a plastic strain direction, $\mathbf{N}$:

$$d\boldsymbol{\varepsilon}^{p} = d\lambda\mathbf{N}. \tag{4}$$

The plastic strain direction is chosen to satisfy the normality condition of the yield locus:

$$f = \left(\boldsymbol{\sigma}' - \sum_{i=1}^{m}\boldsymbol{\alpha}^{(i)}\right):\left(\boldsymbol{\sigma}' - \sum_{i=1}^{m}\boldsymbol{\alpha}^{(i)}\right) - 2k_M{}^2 = 0 \tag{5}$$

where the initial shear yield strength, k_M, scales the difference in the deviatoric and backstress ($\boldsymbol{\alpha}^{(i)}$) terms. The backstress is additively constructed from a multilayer model suggested by Jiang et. al. [12]. The backstress evolution may be expressed in the following format:

$$d\boldsymbol{\alpha}^{(i)} = \left(r^{(i)}\mathbf{N} - \left(\frac{\left\|\boldsymbol{\alpha}^{(i)}\right\|}{r^{(i)}}\right)^{\chi^{(i)}}\boldsymbol{\alpha}^{(i)}\right)c^{(i)}d\lambda \tag{6}$$

where $r^{(i)}$ represents the hardening, $c^{(i)}$ represents an inverse of critical strain, and $\chi^{(i)}$ defines the ratcheting characteristics.

To provide some information on the local stress behavior, the current investigation assumes that the increment in stress is aligned for the elastic and elastic-plastic solutions. Concisely, this condition is written below:

$$\frac{\Delta^{E}\boldsymbol{\sigma}}{\left\|\Delta^{E}\boldsymbol{\sigma}\right\|} = \frac{\Delta\boldsymbol{\sigma}}{\left\|\Delta\boldsymbol{\sigma}\right\|}, \tag{7}$$

where $\Delta^{E}\boldsymbol{\sigma}$ is the increment of stress for the elastic solution, $\Delta\boldsymbol{\sigma}$ is the increment in stress for the elastic-plastic solution, and $\|\mathbf{x}\|$ refers to the 2nd norm of tensor, $\mathbf{x}$, which is defined below for a symmetric 2nd order tensor:

$$\left\|\mathbf{x}\right\| = \sqrt{\mathbf{x}:\mathbf{x}} = \sqrt{x_{11}^2 + x_{22}^2 + x_{33}^2 + 2x_{12}^2 + 2x_{13}^2 + 2x_{23}^2}. \tag{8}$$

This alignment specifies 5 degrees of freedom and is clearly consistent for purely elastic loading, where the two stress definitions should behave identically. Aligning stress direction ensures smoothness in the approximated stress field (for a continuous magnitude estimate), which would maintain equilibrium from the purely elastic solution along with any ‘stress-free’ boundary conditions. This stress alignment is consistent with assuming that the stress concentration factors remain proportional during the elastic-plastic estimate, which is often assumed for engineering applications. This assumption is ideal for fatigue applications, where the critical area is on (or very near) a free surface, which is considered a relatively low constraint. In contrast, components under high constrain (such as those adjacent to relatively rigid material) would benefit from aligning the strain increment, but such scenarios were not considered in this investigation. Furthermore, for general multi-axial loading, both alignments might be overly restrictive (i.e. when stress relaxation results from adjacent plastic strain), but at moderate loads where rate independent plasticity is appropriate, stress redistribution is expected to be negligible.

With the material constitutive model and the elastic to elastic-plastic stress alignment specified, specifying the magnitude of stress would fully characterize the mechanical behavior. More generally, this stress magnitude may be interpreted as a scalar relationship between the purely elastic and elastic-plastic solutions. Fortunately even the earliest works in the notch-problem literature (i.e., Neuber [1] or ESED [2]) provide valuable insight toward constructing this relationship. First consider the equivalent strain energy density (ESED) condition [2-3], which equates the strain energy in the local elastic solution to the local elastic-plastic solution:

$$U_E = U_e + U_p \tag{9}$$

where the purely elastic strain energy, U_E, is decomposed into local elastic (U_e) and plastic (U_p) contributions. Each term is defined by an integral as presented below:

$$\int {}^E\boldsymbol{\sigma} : d^E\boldsymbol{\varepsilon} = \int \boldsymbol{\sigma} : d\boldsymbol{\varepsilon}^e + \int \boldsymbol{\sigma}' : d\boldsymbol{\varepsilon}^p \tag{10}$$

Although the above integrals are well defined for multi-axial cyclic deformation, adjustment is necessary to achieve Masing behavior [13], which is evident in many notch experiments. Specifying Masing behavior is analogous to utilizing a nominal ‘pseudo-material’ to estimate the local elastic-plastic response [9-10]. To clarify this Masing behavior, it is convenient to decompose the elastic strain energy density (U^e) into deviatoric (U_e') and hydrostatic (U_e^{kk}) components, which are defined below:

$$U_e = U_e' + U_e^{kk} \tag{11}$$

where each contribution is easily defined for monotonic loading as:

$$U_e' = \frac{1}{4\mu} \boldsymbol{\sigma}' : \boldsymbol{\sigma}' \tag{12}$$

$$U_e^{kk} = \frac{1}{18\kappa} \left(\mathrm{tr}(\boldsymbol{\sigma})\right)^2 \tag{13}$$

A comparison between the desired Masing behavior and the monotonic solution (Eq. 12) is illustrated for purely deviatoric (i.e., torsion) fully reversed (R = -1) behavior in Figure 1a. As illustrated, U_e' is identical at the endpoints, but varies significantly at intermediate elastic stresses. More specifically, the Masing behavior follows a curve analogous to stress-strain behavior, while the monotonic curve exhibits unique mirrored behavior.

By recognizing the similarity in character to the Masing behavior and the stress-strain response, it is evident that one may adopt a model similar to the plasticity model (Eq. 6) to relate the U^e to the stress. To complete this analogy, consider the monotonic U_e' rewritten to describe the magnitude of deviatoric stress:

$$\|\boldsymbol{\sigma}'\| = 2\sqrt{\mu}\left(U_e'\right)^{\frac{1}{2}} \tag{14}$$

The form of this expression is identical to the common power-law relationship between stress and plastic strain, where the U_e' is replaced with the plastic strain:

$$\sigma = K\left(\varepsilon^p\right)^n \tag{15}$$

Consequentially, the Masing behavior may be achieved for the U_e' by applying a plasticity model with appropriately modified constants. Although this analogy is appropriate, it is more effective to modify the plasticity model to specify the U_e' from a given stress increment. In other words, it is convenient to construct a cyclic pseudo-plasticity model (with kinematic hardening) by a controlled stress increment (rather than plastic strain, or in this case U_e'). To construct such a model, suppose that a stress-energy curve may be described by a series of linear segments, as illustrated in Figure 1. By considering the segments independently (unlike many Armstrong-Frederick type models, which utilize a series of additive segments that are always active prior to saturation [12]), each segment may be uniquely defined in either stress or U_e' space. To take advantage of the known stress-direction stipulated in the current elastic-plastic approximation (Eq. 7), an energy state variable, $\mathbf{q}^{(i)}$, is defined with respect to a stress increment.

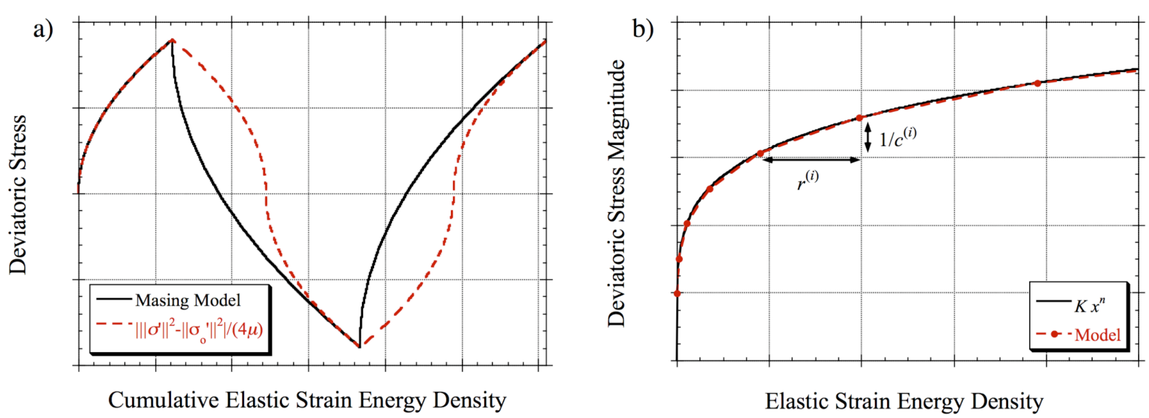

Figure 1: Deviatoric stress magnitude versus (a) cumulative strain energy density for the Masing and monotonic models for fully-reversed cyclic loading and (b) the elastic strain energy density, illustrating the linearly segmented material model

To construct the multi-axial cyclic behavior of a segmented stress-ESED curve (that does not soften or saturate in M terms), each segment is represented by two parameters: the inverse of the increment in deviatoric stress ($c^{(i)}$) and the increment in

U_e' ($r^{(i)}$), both are labeled in Figure 1. Each segment is only activated after the previous segment has achieved saturation ($\left\|\mathbf{q}^{(i-1)}\right\| = r^{(i-1)}$). A 'yield' stress criterion is not necessary, since U_e' would accumulate even at zero stress. Lastly, a rule to prevent saturation was adopted that represents a nearly infinite slope that continues to accumulate U_e' without a (inappropriate) saturation criterion. The evolution of each segmented pseudo-plastic strain was defined similarly to the Jiang et. al. model [12] with an infinite ratcheting exponent. Mathematically, this model may be concisely expressed below separating the two basic conditions:

$$\textit{Hardening:} \quad \left\|\mathbf{q}^{(i-1)}\right\| = r^{(i-1)} \Rightarrow \begin{cases} \left\|\mathbf{q}^{(i)}\right\| < r^{(i)} & \Rightarrow \quad d\mathbf{q}^{(i)} = r^{(i)} c^{(i)} d\boldsymbol{\sigma}' \\ \left\|\mathbf{q}^{(i)}\right\| = r^{(i)} & \Rightarrow \quad d\mathbf{q}^{(i)} = r^{(i)} c^{(i)} d\boldsymbol{\sigma}' - c^{(i)} \left\|d\boldsymbol{\sigma}'\right\| \mathbf{q}^{(i)} \end{cases} \tag{16}$$

$$\textit{Saturation:} \quad \left\|\mathbf{q}^{(M)}\right\| = r^{(M)} \Rightarrow d\mathbf{q}^{(M+1)} = 10^3 r^{(M)} c^{(M)} d\boldsymbol{\sigma}' \tag{17}$$

where the corresponding deviatoric elastic strain energy density is defined as the sum of these state variables projected along the direction of deviatoric stress increment:

$$U_e' = \frac{d\boldsymbol{\sigma}'}{\left\|d\boldsymbol{\sigma}'\right\|} : \sum_{i=1}^{M+1} \left(\mathbf{q}^{(i)}\right) \tag{18}$$

This projection is appropriate since the strain and stress increments are aligned for the elastic deformation (as shown in Eq. 2). It should be noted that this model is not appropriate for plastic deformation, because it bounds plastic strain (instead of back-stress), causing non-physical behavior during multi-axial loading.

The hydrostatic contribution of the ESED should also exhibit Masing behavior. In this case, a 1-D equivalent of the deviatoric model may be forwarded:

$$\textit{Hardening:} \quad \left|q^{(i)}\right| = r^{(i-1)} \Rightarrow \begin{cases} \left|q^{(i)}\right| < r^{(i)} & \Rightarrow \quad dq^{(i)} = r^{(i)} c^{(i)} d\sigma_{kk} \\ \left|q^{(i)}\right| = r^{(i)} & \Rightarrow \quad dq^{(i)} = 0 \end{cases} \tag{19}$$

$$\textit{Saturation:} \quad \left|q^{(M)}\right| = r^{(M)} \Rightarrow dq^{(M+1)} = 10^3 r^{(M)} c^{(M)} d\sigma_{kk} \tag{20}$$

where the constants ($c^{(i)}$ and $r^{(i)}$) are again determined from an expression analogous to Eq. 15:

$$\mathrm{tr}(\boldsymbol{\sigma}) = 3\sqrt{2\kappa}\left(U_{kk}^{e}\right)^{\frac{1}{2}} \tag{21}$$

and the energy is simply the sum of the state variables:

$$U_e^{kk} = \sum_{i=1}^{M} q^{(i)} \tag{22}$$

With Masing behavior adopted to describe the elastic energy (purely elastic and local), fair agreement with experiments is expected. The local plastic strain energy was determined using the usual definition (the last integral in Eq. 10). This definition is appropriate since the plastic behavior already exhibits Masing behavior in the stress-plastic strain response and consequentially the strain energy density when hardening is neglected. Furthermore, an expression analogous to Eq. 14 is not obtainable for the local plastic strain energy density, making using the usual definition a necessity.

Next consider Neuber's [1] condition, which is commonly written as:

$$ {}^{E}\sigma \, {}^{E}\varepsilon = \sigma \varepsilon . \tag{23} $$

This definition also requires significant clarification for applications of multi-axial or cyclic loading criteria (i.e. Masing behavior). In this investigation, it was recognized that the expression in Eq. 23 may be equivalently written by slightly modifying the general ESED expression (Eq. 9). In short, Neuber's condition may be written as:

$$ U_E = U_e + \frac{n+1}{2} U_p , \tag{24} $$

which follows by assuming the classic power-law hardening (Eq. 15) and applying the expressions for monotonic loading (Eqs. 12, 13). In this expression the plastic energy's contribution is decreased (for engineering materials), requiring additional plasticity to achieve the same elastic solution as for the ESED condition. This is consistent with common rule of thumb: the ESED condition predicts lower stresses (i.e. energy) than Neuber's condition, which has been inferred by several authors [7-8]. Furthermore, adopting Eq. 24 allows other cases (besides Neuber and ESED) to be applied without the development of additional Masing models.

RESULTS AND DISCUSSION

The estimation method outlined in the previous section was adopted to predict the deformation behavior of several experiments first conducted by Barkey et. al. [9]. These experiments utilized strain gages at the notch-tip of specimens subjected to nominal axial and torsional multiaxial loading histories. To obtain the local elastic solution based on the nominal loading of these experiments, without a finite element model, one may utilize the concept of stress concentration. For plane stress bi-axial (tension-torsion) loading, the local elastic stress, ${}^{E}\boldsymbol{\sigma}$, may be related to the nominal stress, $\boldsymbol{\xi}$, by the following relationships:

$$ \begin{aligned} {}^{E}\sigma_{zz} &= K_z \, \xi_z = 1.45 \, \xi_z \\ {}^{E}\sigma_{z\theta} &= K_{z\theta} \, \xi_{z\theta} = 1.17 \, \xi_{z\theta} \\ {}^{E}\sigma_{\theta\theta} &= K_z' \xi_z = 0.30 \, \xi_z \end{aligned} \tag{25} $$

where the stress concentration factors K_z, $K_{z\theta}$, and K_z' characterize the notch behavior in the axial, torsion, and transverse directions respectively. The stress concentration factors specified are appropriate for the geometry utilized by Barkey et. al. [9]. The constitutive material behavior was assumed to be isotropic, where the elastic and plastic constants are consistent with the parameters reported in the literature [9]. A summary of these parameters is provided in Table 1, including the Masing elastic strain energy density models, and the Jiang [6] plasticity model.

Table 1: Material parameters for SED and Plasticity models

	Hydrostatic SED $\kappa = 175000$ (MPa)		Deviatoric SED $\mu = 80800$ (MPa)		Plasticity ($\chi^{(i)} = \infty$) $k_M = 139$ (MPa)	
i	$r^{(i)}$ (MPa)	$c^{(i)}$ (MPa^{-1})	$r^{(i)}$ (MPa)	$c^{(i)}$ (MPa^{-1})	$r^{(i)}$ (MPa)	$c^{(i)}$ (-/-)
1	0.020	0.0040	0.191	0.0040	11.8	5200
2	0.050	0.0046	0.480	0.0046	27.0	2930
3	0.079	0.0046	0.769	0.0046	34.2	1510
4	0.109	0.0046	1.060	0.0046	41.6	745
5	0.138	0.0046	1.350	0.0046	49.6	357
6	0.168	0.0046	1.640	0.0046	58.3	169
7	0.198	0.0046	1.930	0.0046	68.2	79.5
8	0.227	0.0046	2.210	0.0046	79.5	37.2
9	0.257	0.0046	2.500	0.0046	92.6	17.4
10	0.287	0.0046	2.790	0.0046	222	8.2

To establish the quality of the estimation method presented in this investigation, both an incremental-step and a 'Box' loading path were employed to compare with the experimental results. The scale of each path was chosen to require moderate plastic deformation in the local 'notch-tip' region of the specimen. First consider the incremental-step path, illustrated in Figure 2a-b. This loading is constructed from a series of cycles with increasing then decreasing magnitude. This history consists of only axial nominal stress, where the other nominal stresses are zero. The nominal axial stress vs. local axial strain is presented in Figure 2a, for the experiment, ESED, and Neuber elastic-plastic approximations. As expected, the Neuber condition predicts higher stresses than the ESED method. Both models provide a reasonable estimate of the experimental results, with the Neuber case providing slightly better agreement. The local stress-strain response is presented in Figure 2b, illustrating that the nominal stress and local stress are on the same order of magnitude. Much higher stresses result from the purely elastic solution, involving the stress concentration factors (Eq. 25). It should be emphasized that this results is not possible without adopted the Masing material behavior to the ESED (i.e., Eqs. 16-17). If Masing is not adopted, similar local response is achieved, but the nominal stress - local strain behavior (Figure 2a) is not reproduced. Instead a non-Masing energy assumption (i.e., Eq. 12) results in a very different response (i.e., a tilted S-shaped curve) for both the ESED and Neuber assumptions.

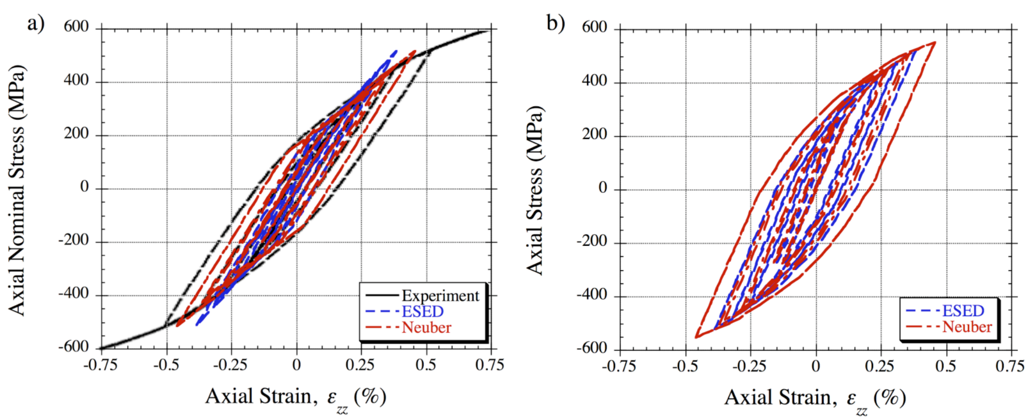

Figure 2: Incremental step test for (a) the nominal stress versus local strain and (b) the local stress versus strain for the experiment [9], ESED and Neuber models

A 'Box' loading path is presented in Figure 3a-b. In this case, the nominal stress response is presented in Figure 3b, where the x-axis is the axial stress (σ_{zz}) and the y-axis is the non-zero torsional stress ($\tau_{z\theta}$). The local strain response is presented in Figure 3a for the experiment, ESED, and Neuber elastic-plastic approximations. As before, both methods provide adequate agreement between the experiment and approximate models. The strain direction deviates from a square box path at the onset of local plasticity for both the experiment and models. Furthermore, the fair agreement in shape suggests that the alignment in directions (Eq. 7) is appropriate, because modifying the direction of loading significantly alters the shape of the local strain response. Lastly, the local stress response is presented in Figure 3b, illustrating the difference in stress magnitude for the ESED and Neuber assumptions. As for the incremental step simulation (Figure 2), the nominal and local stresses are on the same order and have similar character. It should be noted that the purely elastic solution predicts stresses with much higher magnitude, due to the stress concentration factors (Eq. 25).

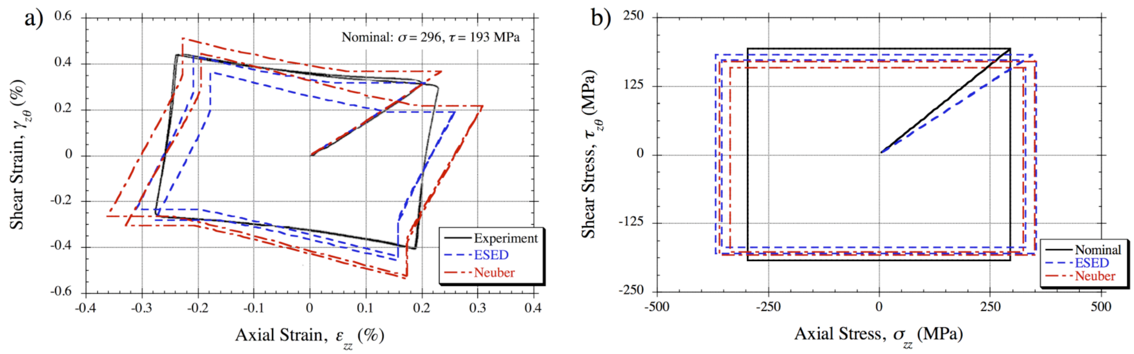

Figure 3: Multiaxial 'Box' loading path illustrating (a) shear strain versus axial strain and (b) the shear stress versus axial stress for the experiment [9], ESED and Neuber models

CONCLUSIONS

The current method to estimate the elastic-plastic response from a purely elastic history decouples the notch geometry and local material response by utilizing a modified boundary condition approach. Specifically, the method combines a magnitude criterion with directional alignment to impose boundary conditions for an appropriate multiaxial plasticity model. The assumptions of the current construct are developed in a general manner, with the potential to adjust the constraint (direction alignment, i.e. stress), magnitude (i.e. ESED or Neuber), and the plasticity character. A few additional conclusions may be drawn:

- Because of the representation the elastic strain energy density, the current method exhibits Masing behavior between the nominal stress and local strain consistently with the experimental evidence.
- Multiaxial experimental results were adequately reproduced based on the material's notch-free mechanical behavior (a stress-strain curve), geometrically determined stress concentration factors, and a choice of magnitude criteria (ESED or Neuber).

- With appropriate modeling choices, the current approach should be consistent with any arbitrary multiaxial cyclic loading. Subsequently, the elastic-plastic response may be employed to improve fatigue life or damage estimates associated with the local mechanical response.

REFERENCES

[1] Neuber, H. "Theory of stress concentration for shear-strained prismatical bodies with arbitrary non-linear stress-strain law." *ASME J. Appl. Mech.* **28** (1961): 544-550.

[2] Molski, K. and G. Glinka. "A method of elastic-plastic stress and strain calculation at a notch root." *Materials Science and Engineering,* **50** (1981): 93-100.

[3] Glinka, G. "Energy density approach to calculation of inelastic strain-stress near notches and cracks." *Engineering Fracture Mechanics,* **22.3** (1985): 485-508.

[4] Moftakhar, A., A. Buczynski and G. Glinka. "Calculation of elasto-plastic strains and stresses in notches under multiaxial loading." *International Journal of Fracture*, **70** (1995): 357-373.

[5] Hoffmann, M. and T. Seeger. "A generalized method for estimating multiaxial elastic-plastic notch stresses and strains part 1: theory." *Journal of Engineering Materials and Technology,* **107** (1985): 250-254.

[6] Shatil, G., E. G. Ellison, and D. J. Smith. "Elastic-plastic behavior and uniaxial low cycle fatigue life of notched specimens." *Fatigue Fract. Engng. Mater. Struct.,* **18.2** (1995): 235-245.

[7] Sharpe, W. N., C. H. Yang Jr., and R. L. Tregoning. " An evaluation of the Neuber and Glinka relations for monotonic loading." *ASME J. Appl. Mech.,* **59** (1992): 50-56.

[8] Adibi-Asl, R. and R. Seshadri. "Improved prediction method for estimating notch elastic-plastic strain." *Journal of Pressure Vessel Technology,* **132** (2010): 011401-1-8.

[9] Barkey, M. E., D. F. Socie, and K. J. Hsia. "A yield surface approach to the estimation of notch strain for proportional and nonproportional cyclic loading." *Journal of Engineering Materials and Technology,* **116** (1994): 173-180.

[10] Köttgen, V. B., M. E. Barkey, and D. F. Socie. "Pseudo stress and pseudo strain based approaches to multiaxial notch analysis." *Fatigue Fract. Engng. Mater. Struct.,* **18.9** (1995): 981-1006.

[11] Hosford, W. F. *Mechanical behavior of materials.* New York: Cambridge University Press, 2005.

[12] Jiang, Y. and P. Kurath. "Characteristics of the Armstrong-Frederick type plasticity models." *International Journal of Plasticity,* **12.3** (1996): 387-415.

[13] Suresh, S. *Fatigue of Materials.* Cambridge: Cambridge University Press, 1998.